This article has been accepted for publication in a future issue of this journal, but has not been fully edited. Content may change prior to final publication. Citation information: DOI 10.1109/LAWP.2015.2422571, IEEE Antennas and Wireless Propagation Letters

Compact Offset Microstrip-fed MIMO Antenna for Band-Notched UWB Applications

Le Kang, Hui Li, Xinhuai Wang, and Xiaowei Shi

***Abstract*—A compact multiple-input–multiple-output (MIMO) antenna is presented for ultrawideband (UWB) applications with band-notched function. The proposed antenna is composed of two offset microstrip-fed antenna elements with UWB performance. To achieve high isolation and polarization diversity, the antenna elements are placed perpendicular to each other. A parasitic T-shaped strip between the radiating elements is employed as a decoupling structure to further suppress the mutual coupling. In addition, the notched band at 5.5 GHz is realized by etching a pair of L-shaped slits on the ground. The antenna prototype with a compact size of 38.5 × 38.5 mm^2 has been fabricated and measured. Experimental results show that the antenna has an impedance bandwidth of 3.08-11.8 GHz with reflection coefficient less than -10 dB, except the rejection band of 5.03-5.97 GHz. Besides, port isolation, envelope correlation coefficient and radiation characteristics are also investigated. The results indicate that the MIMO antenna is suitable for band-notched UWB applications.**

***Index Terms*—Band-notched, multiple-input–multiple-output (MIMO) antenna, offset microstrip-fed, ultrawideband (UWB) antenna.**

I. Introduction

SINCE the Federal Communication Commission (FCC) released the spectrum from 3.1 to 10.6 GHz for commercial applications [1], ultrawideband (UWB) techniques have drawn considerable attention due to the merits such as wide bandwidth, high data rate, and low cost. UWB antennas, as one of the key components of UWB wireless communication system, have been widely investigated. Although UWB communication system makes use of huge frequency bands, the permitted power spectral density of the UWB signal is rather limited to avoid interference with other systems [2]. The multiple-input multiple-output (MIMO) techniques enable the transmission of data over multiple channels, and thus increase the channel capacity without additional power requirements [3]. Besides, MIMO antennas can be used for achieving diversity performance and mitigating the effects of multipath fading [4].

The use of multi-element antennas can effectively increase the channel capacity and improve the reliability of UWB wireless communications. However, strong mutual coupling caused between the antenna elements will deteriorate the performance of UWB MIMO system. Hence, isolation enhancement becomes one of the main challenges in MIMO antenna designs. Until now, various types of decoupling techniques have been reported [5]-[10]. In [5]-[8], the mutual coupling can be reduced by adopting different decoupling elements, such as the tree-like [7] and floating parasitic [8] structures. However, the structures in [7] and [8] occupy much space and make the antenna configuration more complex. Diversity antennas are also a promising choice in achieving low mutual coupling between antenna elements owing to the orthogonal radiation patterns [9], [10]. Moreover, in order to reject the interference with the existing wireless communication systems such as the Wireless Local Area Networks (WLAN) operating at 5.15-5.85 GHz, antennas are required to filter out the undesired band. Recently, several UWB MIMO antennas with band-reject operation have been presented [11]-[13]. The band-notched characteristics are realized by introducing an arc shaped slot [11], a split-ring resonator (SRR) slot [12] and an open stub [13] in the antenna element, respectively. Though good performance can be obtained, the smallest dimension of the antennas with an area of 48 × 48 mm^2 [12] is larger than that of the proposed antenna.

In this letter, a compact band-notched UWB MIMO antenna with two identical antenna elements is proposed and analyzed. The antenna element with a rhombic slot is fed by an offset microstrip-fed line. Compared with the conventional center-fed slot antennas, the offset microstrip-fed slot antenna can provide a broader impedance bandwidth [14]. The orthogonally fed MIMO antenna achieves not only polarization diversity but also high isolation. Moreover, a parasitic T-shaped strip is introduced between the antenna elements to further reduce the mutual coupling and a pair of L-shaped slits are etched on the ground to generate a notched band. Meanwhile, the proposed antenna occupies a small area of 38.5 × 38.5 mm^2. Details of antenna design and both the simulated and measured results are presented in the following sections.

II. Antenna Design

A. Antenna Configuration

Fig. 1 illustrates the geometry of the proposed band-notched UWB MIMO antenna. The designed antenna with an overall size of 38.5 × 38.5 mm^2 is printed on an FR4 substrate with a thickness of 1.6 mm and a relative dielectric constant of 4.4. It consists of two orthogonal microstrip-fed lines, a parasitic T-shaped strip, and a ground plane etched with a rhombic slot and a pair of L-shaped slits. Both the microstrip-fed lines at an offset distance from the center have three stages for impedance

This work was supported by the natural science foundation of Shaanxi Province under Grant 2014JQ8350 and by the funds for Space TT & C communication innovation and exploration under Grant SMC1401.

The authors are with the Science and Technology on Antenna and Microwave Laboratory, Xidian University, Xi'an 710071, China (e-mail: Lkang@xidian.edu.cn).

1536-1225 (c) 2015 IEEE. Personal use is permitted, but republication/redistribution requires IEEE permission. See http://www.ieee.org/publications_standards/publications/rights/index.html for more information.

This article has been accepted for publication in a future issue of this journal, but has not been fully edited. Content may change prior to final publication. Citation information: DOI 10.1109/LAWP.2015.2422571, IEEE Antennas and Wireless Propagation Letters

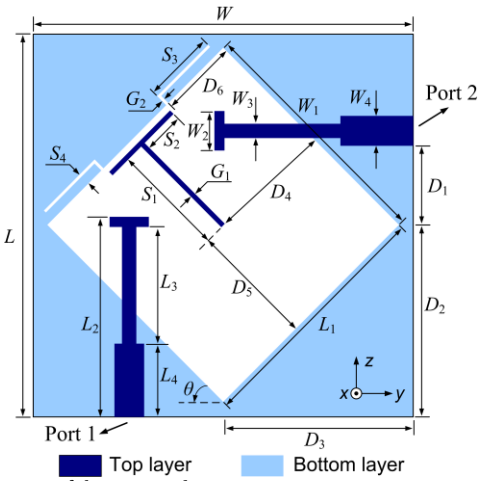

Fig. 1. Geometry of the proposed antenna.

transforming. The parasitic strip placed between the antenna elements plays an important role in isolation improvement. It consists of two major parts: a strip along the diagonal and the other perpendicular to the diagonal. The ground plane is designed on the other side of the substrate. The slits etched on the ground are used to produce a notched band at 5.5 GHz. The numerical analysis and geometry refinement of the antenna structure were carried out by using electromagnetic simulation software HFSS from ANSYS. The optimal parameters are recorded as follows (in millimeters): $W = L = 38.5$, $W_1 = L_1 = 25.2$, $W_2 = 4$, $W_3 = 1.5$, $W_4 = 3$, $L_2 = 20.4$, $L_3 = 12$, $L_4 = 7.4$, $D_1 = 8$, $D_2 = D_3 = 19.25$, $D_4 = 12.35$, $D_5 = 12.6$, $D_5 = 7.8$, $G_1 = 0.5$, $G_2 = 0.3$, $S_1 = 11.5$, $S_2 = 4.15$, $S_3 = 7.3$, $S_4 = 1.3$, and $\theta = 45$ °.

B. Design of UWB Antenna Element

Fig. 2 shows the design evolution of UWB antenna elements with different feeding structures. Compared with the center-fed printed antenna with a rhombic slot (denoted as Ant. 1), good impedance matching over a wider frequency range can be achieved by adopting an offset microstrip-fed line (denoted as Ant. 2). This is due to the fact that the electromagnetic coupling between the feed line and the ground improves as the microstrip line is shifted from the center, and thereby enhances the impedance bandwidth of the antenna. The offset distance D_1 has a significant influence on the impedance enhancement of the antenna element, and an optimum value D_1 = 8 mm is selected in this design. The feed lines of Ant. 1 and 2 both have the same widths of 3 mm corresponding to 50-Ω characteristic impedance. Then a three-stage feed line is employed as an impedance transformer to adjust the impedance matching at 5-8 GHz (denoted as Ant. 3). Finally, an impedance bandwidth of larger than 3.1-10 GHz can be obtained to meet the bandwidth requirement for UWB operation.

C. Effects of Parasitic Strip and Etched Slits

The simulated S-parameters of the MIMO antennas with different configurations are given in Fig. 3. As can be seen, the basic UWB-MIMO antenna with orthogonal feeding structures achieves port isolation of better than -10 dB in the UWB spectrum. To further improve the isolation, a parasitic T-shaped strip is added between the antenna elements as a decoupling

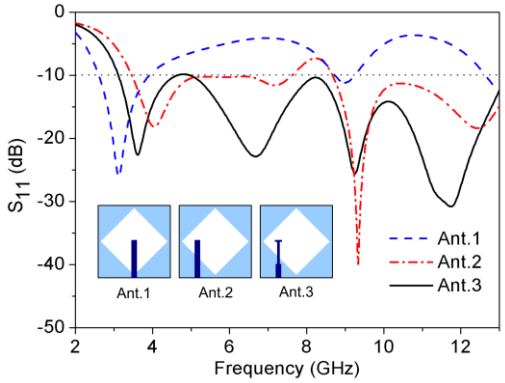

Fig. 2. Design evolution of the UWB antenna elements.

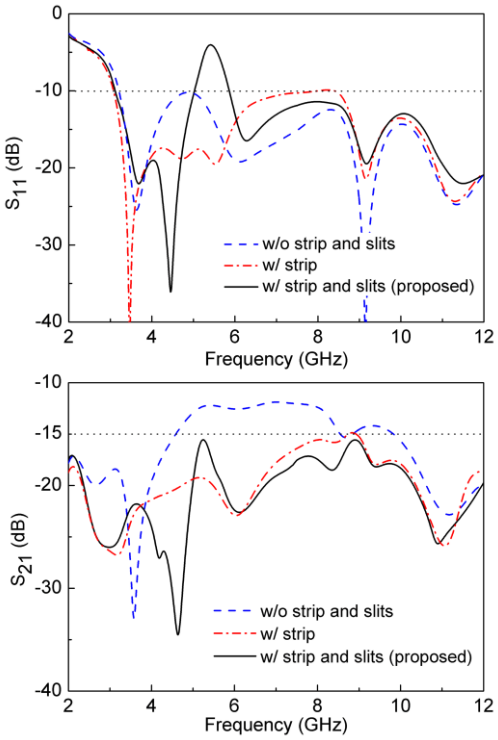

Fig. 3. Simulated S-parameters of the MIMO antennas with different configurations.

structure. The strip acts as a parasitic resonator, which provides an additional coupling path to counteract the current coupled directly from one antenna element on the other [5], [6].

To investigate the influence of the T-shaped strip, the surface current distributions at 6.0 GHz are shown in Fig. 4, in which Port 1 is excited and Port 2 is terminated with a 50-Ω load. Without the strip, strong coupled current can be observed on the right antenna element, which flows in the direction opposite to that of the current along the left antenna element. With a total length of 15.6 mm (S_1+S_2), the strip can excite a half-wavelength resonant mode at about 6.0 GHz. By adopting the parasitic structure, larger surface current is induced along the strip and an additional coupling path is created between the adjacent elements through the strip. Since this coupling path can produce reverse current to cancel out the original coupling. The current coupled on the right antenna element decreases substantially and hence the mutual coupling at 4.6-8.5 GHz is

1536-1225 (c) 2015 IEEE. Personal use is permitted, but republication/redistribution requires IEEE permission. See http://www.ieee.org/publications_standards/publications/rights/index.html for more information.

This article has been accepted for publication in a future issue of this journal, but has not been fully edited. Content may change prior to final publication. Citation information: DOI 10.1109/LAWP.2015.2422571, IEEE Antennas and Wireless Propagation Letters

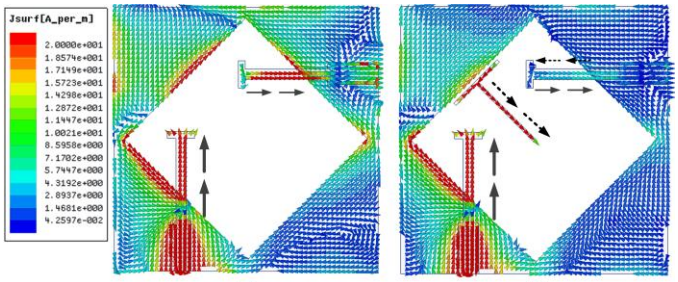

(a) (b)

Fig. 4. Simulated current distributions at 6.0 GHz (a) without the T-shaped strip and (b) with the T-shaped strip.

reduced to less than -15 dB with little effect on the impedance matching.

The pair of open-ended slits etched on the ground are employed to generate band-notched function. The notched band can be controlled by adjusting the lengths of the slits. It is found that the total length of each slit is taken as 8.6 mm (S_3+S_4), which is about a quarter of the guided wavelength at 5.5 GHz. Therefore, a notched band of 5-5.9 GHz can be generated to reject the 5.2/5.8-GHz WLAN operation.

III. Results and Discussions

A. S-Parameters

The antenna prototype shown in Fig. 5 was measured with the Agilent N5244A vector network analyzer. Fig. 6 presents the simulated and measured S-parameters against frequency. Measured results show that the antenna provides an impedance bandwidth (S_{11} & $S_{22} \leq$ -10dB) from 3.08 to 11.8 GHz except the notched band of 5.03-5.97 GHz. Thus, the bandwidth requirement for UWB applications is satisfied, and band-notched function is achieved to avoid the potential interference of 5.2/5.8-GHz WLAN operation. It also can be seen that the measured port isolations (S_{21} & S_{12}) are below -15 dB throughout the whole UWB band. Due to the effects of manufacturing tolerance and measurement environment, measured port isolation is slightly worse than the simulation at lower frequencies from 3 to 5.5 GHz. In MIMO systems, mutual coupling of better than -15 dB is considered to be acceptable for practical applications.

B. Radiation Characteristics

The radiation characteristics of the proposed antenna have been measured with Port 1 or 2 excited. Measured radiation patterns (*xoy*-, *xoz*-, and *yoz*-planes) at 3.5, 7.5, and 9.5 GHz are plotted in Fig. 7. Since the MIMO antenna consists of two identical elements located perpendicular to each other, the patterns of Port 1 and 2 are almost similar with a 90 °rotation. As observed, the radiation patterns are quasi-omnidirectional in the *H*-plane (*xoy*-plane of Port 1 and *xoz*-plane of Port 2). The asymmetric antenna structure contributes to the high-level cross polarizations of the radiation patterns. However, the MIMO antenna can still achieve orthogonal patterns to mitigate the effect of coupling between the adjacent elements. Fig. 8 shows the measured peak gains and radiation efficiencies of the antenna with one port excited. Measured peak gains range from

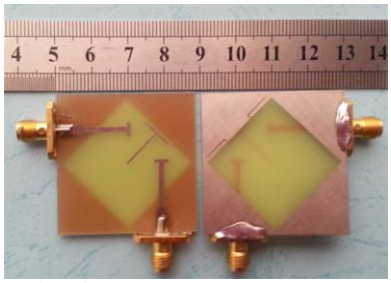

Fig. 5. Photograph of the fabricated antenna.

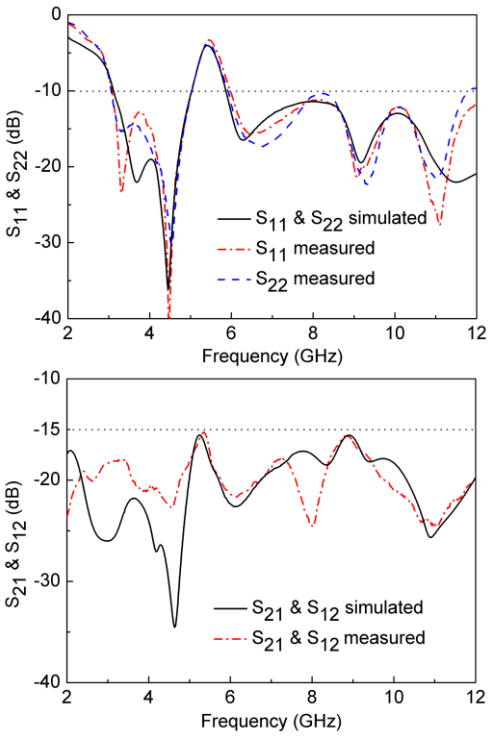

Fig. 6. Simulated and measured S-parameters of the proposed antenna.

1.4 to 3.6 dBi throughout the entire band except the notched point where it drops to -4.5 dBi. The radiation efficiencies are above 75% in the UWB spectrum, while it drops to about 34% at the notched frequency of 5.5 GHz.

C. Diversity Performance

An important parameter used to evaluate diversity performance in MIMO systems is the envelope correlation coefficient (ECC). For two-port antenna diversity systems, an approach that requires neither the computation nor the measurement of the radiation pattern is presented by computing the envelope correlation [15]. Based on the S-parameters, the ECC can be calculated as:

$$\rho_e = \frac{|S_{11}^* S_{12} + S_{21}^* S_{22}|^2}{(1-|S_{11}|^2-|S_{21}|^2)(1-|S_{22}|^2-|S_{12}|^2)} \quad (1)$$

Fig. 9 displays the simulated and measured ECC curves. It is obvious that both the simulated and measured results are below 0.02 across the UWB band from 3.1 to 10.6 GHz, which proves that the proposed MIMO antenna is suitable for diversity systems.

1536-1225 (c) 2015 IEEE. Personal use is permitted, but republication/redistribution requires IEEE permission. See http://www.ieee.org/publications_standards/publications/rights/index.html for more information.

This article has been accepted for publication in a future issue of this journal, but has not been fully edited. Content may change prior to final publication. Citation information: DOI 10.1109/LAWP.2015.2422571, IEEE Antennas and Wireless Propagation Letters

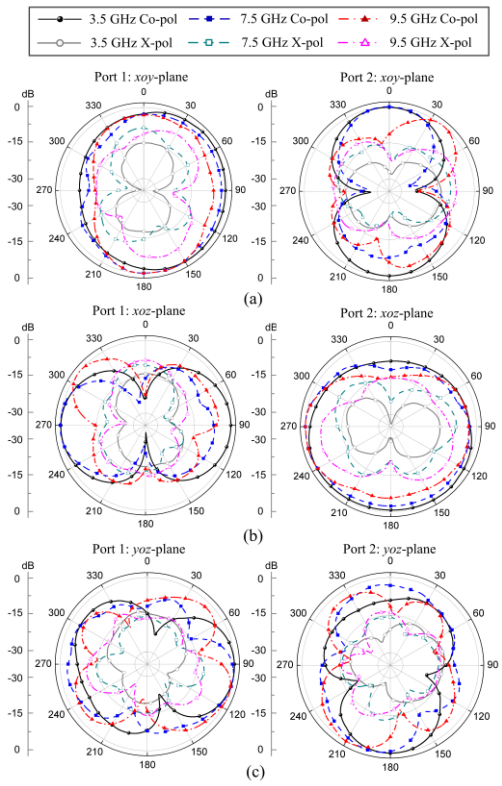

Fig. 7. Measured radiation patterns of the proposed antenna at 3.5, 7.5, and 9.5 GHz: (a) *xoy*-plane, (b) *xoz*-plane, and (c) *yoz*-plane.

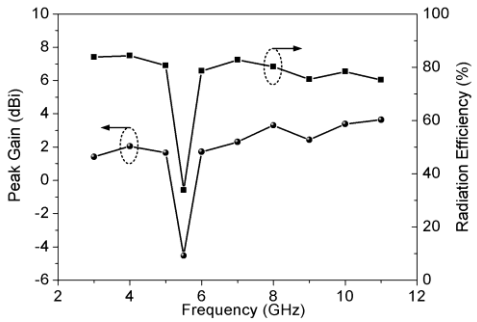

Fig. 8. Measured gains and radiation efficiencies of the proposed antenna.

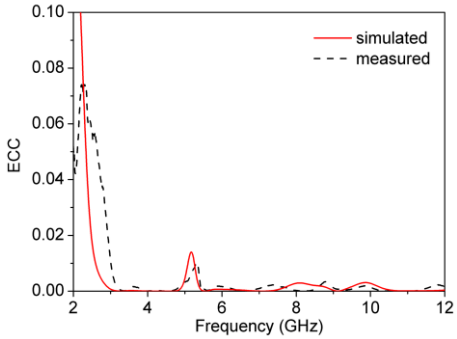

Fig. 9. Simulated and measured envelope correlation coefficients of the proposed antenna.

IV. Conclusion

A UWB MIMO antenna with band-notched characteristics is presented. The offset microstrip-fed lines are employed to feed the antenna with wideband impedance matching. Port isolation is improved by using a simple decoupling structure. Measured results show that the proposed antenna achieves an impedance bandwidth of larger than 3.1–10.6 GHz except sharp rejection band of 5.03-5.97 GHz. Besides, low mutual coupling of better than -15 dB and low envelope correlation coefficient of less than 0.02 can also be obtained through the whole UWB band. With the features mentioned above and a compact size, the proposed antenna can be a promising candidate for MIMO/diversity systems.

References

[1] Federal Communications Commission, Washington, DC, USA, "Federal Communications Commission revision of Part 15 of the Commission's rules regarding ultra-wideband transmission system from 3.1 to 10.6 GHz," ET-Docket, 2002, pp. 98–153.

[2] T. Kaiser, F. Zheng, and E. Dimitrov, "An overview of ultra-wide-band systems with MIMO," *Proc. IEEE*, vol. 97, no. 2, pp. 285–312, Feb. 2009.

[3] J. Wallace, M. Jensen, A. Swindlehurst, and B. Jeffs, "Experimental characterization of the MIMO wireless channel: Data acquisition and analysis," *IEEE Trans. Wireless Commun.*, vol. 2, no. 2, pp. 335–343, Mar. 2003.

[4] X. Wang, Z. H. Feng, and K. M. Luk, "Pattern and polarization diversity antenna with high isolation for portable wireless devices," *IEEE Antennas Wireless Propag. Lett.*, vol. 8, pp.209-211, 2009.

[5] A. C. K. Mak, C. R. Rowell, and R. D. Murch, "Isolation enhancement between two closely packed antennas," *IEEE Trans. Antennas Propag.*,vol. 56, no. 11, pp. 3411–3419, Nov. 2008.

[6] Z. Y. Li, Z. W. Du, M. Takahashi, K. Saito, and K. Ito, "Reducing mutual coupling of MIMO antennas with parasitic elements for mobile terminals," *IEEE Trans. Antennas Propag.*, vol. 60, no. 2, pp. 473–481, Feb. 2012.

[7] M. S. Khan *et al.*, "Compact ultra-wideband diversity antenna with a floating parasitic digitated decoupling structure," *Microw., Antennas Propag.*, vol. 8, no. 10, pp. 747–753, Jul. 2014.

[8] S. Zhang, Z. Ying, J. Xiong, and S. He, "Ultrawideband MIMO/diversity antennas with a tree-like structure to enhance wideband isolation," *IEEE Antennas Wireless Propag. Lett.*, vol. 8, pp. 1279–1282, 2009.

[9] M. Gallo *et al.*, "A broadband pattern diversity annular slot antenna," *IEEE Trans. Antennas Propag.*, vol. 60, no. 3, pp. 1596–1600, Mar. 2012.

[10] J. Ren, W. Hu, Y. Z. Yin, and R. Fan, "Compact printed MIMO antenna for UWB applications," *IEEE Antennas Wireless Propag. Lett.*, vol. 13, pp. 1517–1520, 2014.

[11] B. P. Chacko, G. Augustin, and T. A. Denidni, "Uniplanar polarisation diversity antenna for ultrawideband systems," *Microw., Antennas Propag.*, vol. 7, no. 10, pp. 854–857, Jul. 2013.

[12] P. Gao *et al.*, "Compact printed UWB diversity slot antenna with 5.5-GHz band-notched characteristics," *IEEE Antennas Wireless Propag. Lett.*, vol. 13, pp. 376–379, 2014.

[13] J.-M. Lee, K.-B. Kim, H.-K. Ryu, and J.-M. Woo, "A compact ultrawideband MIMO antenna with WLAN band-rejected operation for mobile devices," *IEEE Antennas Wireless Propag. Lett.*, vol. 11, pp. 990–993, 2012.

[14] J.-Y. Jan, and J.-C. Kao, "Novel printed wide-band rhombus-like slot antenna with an offset microstrip-fed line," *IEEE Antennas Wireless Propag. Lett.*, vol. 6, pp. 249–251, 2007.

[15] S. Blanch, J. Romeu, and I. Corbella, "Exact representation of antenna system diversity performance from input parameter description," *Electron. Lett.*, vol. 39, no. 9, pp. 705–707, May 2003.

1536-1225 (c) 2015 IEEE. Personal use is permitted, but republication/redistribution requires IEEE permission. See http://www.ieee.org/publications_standards/publications/rights/index.html for more information.